Cell Metabolism
Article

T Lymphocytes Amplify the Anabolic Activity of Parathyroid Hormone through Wnt10b Signaling

Masakazu Terauchi,[1,10] Jau-Yi Li,[1,10] Brahmchetna Bedi,[1] Ki-Hyun Baek,[1] Hesham Tawfeek,[1] Sarah Galley,[1] Linda Gilbert,[5] Mark S. Nanes,[1,5] Majd Zayzafoon,[6] Robert Guldberg,[7] David L. Lamar,[2] Meredith A. Singer,[8] Timothy F. Lane,[8] Henry M. Kronenberg,[9] M. Neale Weitzmann,[1,3,5] and Roberto Pacifici[1,4,*]
[1]Division of Endocrinology, Metabolism, and Lipids, Department of Medicine
[2]Kathleen B. and Mason I. Lowance Center for Human Immunology, Department of Medicine
[3]Emory Winship Cancer Institute
[4]Immunology and Molecular Pathogenesis Program
Emory University, Atlanta, GA 30322, USA
[5]Atlanta VA Medical Center, Decatur, GA 30033, USA
[6]Department of Pathology, The University of Alabama at Birmingham, Birmingham, AL 35294, USA
[7]Woodruff School of Mechanical Engineering, Georgia Institute of Technology, Atlanta, GA 30332, USA
[8]Department of Obstetrics and Gynecology, Department of Biological Chemistry, and Orthopedic Hospital Research Center, University of California, Los Angeles, Los Angeles, CA 90095, USA
[9]Endocrine Unit, Massachusetts General Hospital, Boston, MA 02114, USA
[10]These authors contributed equally to this work
*Correspondence: roberto.pacifici@emory.edu
DOI 10.1016/j.cmet.2009.07.010

SUMMARY

Intermittent administration of parathyroid hormone (iPTH) is used to treat osteoporosis because it improves bone architecture and strength, but the underlying cellular and molecular mechanisms are unclear. Here, we show that iPTH increases the production of Wnt10b by bone marrow CD8+ T cells and induces these lymphocytes to activate canonical Wnt signaling in preosteoblasts. Accordingly, in responses to iPTH, T cell null mice display diminished Wnt signaling in preosteoblasts and blunted osteoblastic commitment, proliferation, differentiation, and life span, which result in decreased trabecular bone anabolism and no increase in strength. Demonstrating the specific role of lymphocytic Wnt10b, iPTH has no anabolic activity in mice lacking T-cell-produced Wnt10b. Therefore, T-cell-mediated activation of Wnt signaling in osteoblastic cells plays a key permissive role in the mechanism by which iPTH increases bone strength, suggesting that T cell osteoblast crosstalk pathways may provide pharmacological targets for bone anabolism.

INTRODUCTION

Sustained overproduction or in vivo continuous delivery of parathyroid hormone (PTH) is a cause of bone loss (Grey et al., 1996; Potts, 1998). However, when injected daily, a regimen known as intermittent PTH treatment, the hormone markedly stimulates trabecular and cortical bone formation. Although this bone-forming activity is antagonized, in part, by a stimulation of bone resorption, the net effect of intermittent PTH treatment is an improvement in bone microarchitecture and increased strength (Qin et al., 2004; Zaidi, 2007). As a result, intermittent treatment with the 1–34 fragment of PTH is an FDA-approved treatment modality for postmenopausal osteoporosis (Neer et al., 2001).

PTH promotes bone formation by increasing the number of osteoblasts (OBs) through multiple effects, including activation of quiescent lining cells (Dobnig and Turner, 1995), increased OB proliferation (Nishida et al., 1994; Pettway et al., 2007) and differentiation (Nishida et al., 1994; Schmidt et al., 1995), and attenuation of pre-OB and OB apoptosis (Almeida et al., 2005; Bellido et al., 2003; Jilka et al., 1999). However, the specific contribution of each of these effects to the overall anabolic activity of PTH remains controversial.

PTH binds to the PTH/PTH-related protein (PTHrP) receptor (PPR or PTH-1R), which is expressed on OBs, osteocytes, and bone marrow (BM) stromal cells (SCs) (Calvi et al., 2001; Qin et al., 2004). Ligand binding to PPR activates the cyclic AMP-dependent protein kinase A and calcium-dependent protein kinase C signaling pathways (Gensure et al., 2005; Jilka, 2007).

PTH signaling has been observed to intersect Wnt pathways in OBs. Activation of Wnt signaling induces OB proliferation (Kato et al., 2002) and differentiation (Bodine and Komm, 2006), prevents OB apoptosis (Almeida et al., 2005; Bodine et al., 2005), and augments OB production of OPG (Glass et al., 2005), a soluble decoy receptor for the osteoclastogenic cytokine RANKL. Wnt proteins initiate a canonical signaling cascade by binding to receptors of the Frizzled family together with coreceptors, members of the low-density lipoprotein receptor-related protein (LRP) family, LRP5 and LRP6, which results in the stabilization of cytosolic β-catenin. Interaction of β-catenin with transcription factors of the lymphoid-enhancer-binding factor/T cell factor family in the nucleus subsequently regulates the transcription of Wnt target genes (Behrens et al., 1996). Wnt signaling plays a critical role in bone formation, as inactivating mutations of LRP5 cause osteoporosis in humans (Behrens et al., 1996) and low bone mass in mice (Kato et al., 2002).

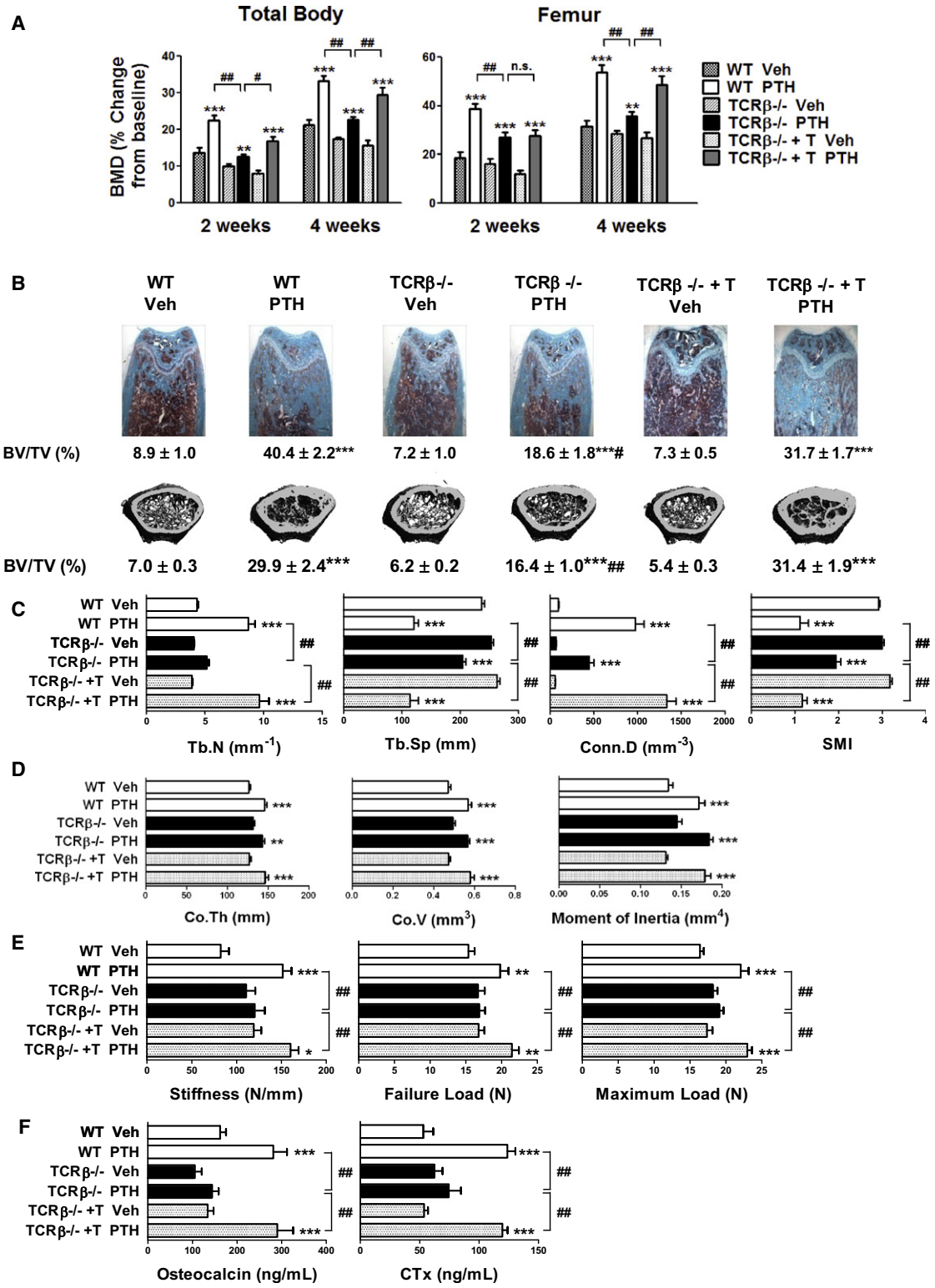

Figure 1. Analysis of the Effects of iPTH Treatment in WT Mice, *TCR*β$^{-/-}$ Mice, and *TCR*β$^{-/-}$ Mice Previously Subjected to Adoptive Transfer of WT T Cells

(A) In vivo total body and femoral BMD measurements by DXA at 2 and 4 weeks of treatment.

(B) Femoral histology and ex vivo μCT analysis of femoral trabecular bone. Representative longitudinal histological sections stained by Goldner's Trichrome stain, cross-sectional μCT reconstructions, and trabecular bone volume (BV/TV) measured by bone histomorphometry and μCT are shown.

PTH is a canonical Wnt signaling agonist that increases β-catenin levels in osteoblastic cells (Kulkarni et al., 2005), an effect that occurs through modulation of both the protein kinase A and protein kinase C pathways (Tobimatsu et al., 2006). PTH, once bound to PPR, is also capable of forming a complex with LRP6 that results in LRP6 signaling and β-catenin activation (Wan et al., 2008). Thus, PTH activates Wnt signaling in osteoblastic cells through both Wnt ligands' dependent and independent mechanisms. Moreover, PTH downregulates the production of sclerostin, an osteocyte-derived Wnt-signaling antagonist (Bellido et al., 2005), Dickkopf-1, a soluble LRP5- and LRP6-signaling inhibitor (Kulkarni et al., 2005), and Sfrp-4, a factor that binds Wnt proteins, thus antagonizing both canonical and noncanonical Wnt signaling (Qin et al., 2003).

These reports suggest that Wnt signaling in cells of the osteoblastic lineage plays a role in PTH-induced anabolism. However, uncertainty remains with regard to the relevance of canonical Wnt signaling in the mode of action of PTH, as the silencing of LRP5 does not abrogate trabecular bone anabolism (Iwaniec et al., 2007; Sawakami et al., 2006). Furthermore, the identity and source of Wnt ligands that activate Wnt signaling in response to PTH treatment are not completely known.

Though SCs, OBs, and osteocytes represent the major targets of PTH in bone, accessory cells that express PPR may play a contributory or permissive role. Among them are T lymphocytes, a lineage that responds to PTH (Geffner et al., 1995; Stojceva-Taneva et al., 1993), stimulates OB differentiation (Rifas et al., 2003), and expresses Wnt10b (Hardiman et al., 1996; Ouji et al., 2006), a Wnt ligand produced in the BM that inhibits adipogenesis and stimulates osteoblastogenesis (Bennett et al., 2005). We have reported that a continuous infusion of PTH fails to induce bone resorption and cortical bone loss in mice lacking T cells (Gao et al., 2008). This is because T cells increase the capacity of SCs to support PTH-induced osteoclastogenesis through CD40L, a surface molecule of activated T cells that induces CD40 signaling in osteoblastic cells (Gao et al., 2008). Although T cells in that study were found not to be required for continuous PTH treatment to stimulate bone formation, little information is available on whether T cells contribute to the anabolic response to intermittent PTH.

In the present studies, we report that intermittent PTH treatment increases the production of Wnt10b by BM CD8+ cells and that deletion of T cells, or T-cell-expressed Wnt10b, results in blunted trabecular bone anabolism.

RESULTS

T-Cell-Deficient Mice Exhibit a Blunted Anabolic Response to iPTH

To determine whether T lymphocytes are required for intermittent PTH to exert its effects on bone, 5-week-old wild-type (WT) and congenic *TCR*$\beta^{-/-}$ mice, a strain completely devoid of αβ T cells, were injected daily with vehicle or 80 μg/kg of hPTH 1–34 for 4 weeks, a treatment modality referred to hereafter as iPTH. To control for strain-dependent confounders, the study included *TCR*$\beta^{-/-}$ mice subjected to adoptive transfer of WT T cells 1 week before initiation of iPTH treatment, a procedure that is followed by the engraftment and homeostatic expansion of the donor T cells (Gao et al., 2007; Roggia et al., 2001). Dual X-ray absorptiometry (DXA) was utilized to measure in vivo total body and femoral bone mineral density (BMD). At baseline, WT and *TCR*$\beta^{-/-}$ mice had similar BMD values (Figure S1 available online). Due to growth, BMD increased in all vehicle-treated groups during the 4 weeks of the experiment (Figure 1A). In WT and T-cell-reconstituted *TCR*$\beta^{-/-}$ mice, iPTH induced a ~55%–~85% greater increase in the total body BMD and a ~70%–~80% greater gain in femur BMD, as compared to vehicle. Conversely, in T-cell-deficient *TCR*$\beta^{-/-}$ mice, iPTH augmented total body and femur BMD only ~30% and ~25% more than vehicle, respectively.

Cancellous bone was analyzed by histology and microcomputed tomography (μCT), utilizing femurs that were harvested at sacrifice. Histomorphometric measurements of trabecular bone volume (BV/TV) revealed a less-pronounced anabolic response to PTH in *TCR*$\beta^{-/-}$ mice than in controls (Figure 1B). μCT analysis showed that iPTH increased in all groups. However, BV/TV was ~46%–~48% lower in iPTH-treated *TCR*$\beta^{-/-}$ mice, as compared to iPTH-treated WT and T-cell-reconstituted controls. Parameters of trabecular structure (Figure 1C) were also differentially affected in T-cell-deficient and T-cell-replete mice, as trabecular number (Tb.N), trabecular separation (Tb.Sp), connectivity density (Conn.D), and structure model index (SMI) were more substantially improved in WT and reconstituted mice than in *TCR*$\beta^{-/-}$ mice.

By contrast, μCT analysis of cortical bone showed that iPTH induced similar increases in cortical thickness (Co.Th), cortical volume (Co.V), and moment of inertia in all groups of mice (Figure 1D), thus demonstrating that T cells specifically augment the capacity of iPTH to improve architecture in trabecular bone.

Analysis of femoral structural properties by four-point bending tests revealed that iPTH increased stiffness, failure load, and maximum load in WT mice and T-cell-reconstituted *TCR*$\beta^{-/-}$ mice, but not in T-cell-deficient *TCR*$\beta^{-/-}$ mice (Figure 1E). As structural properties reflect the strength of the whole bone, these findings demonstrate that lack of T cells blunts iPTH-induced trabecular anabolism by a degree sufficient to hamper the improvement in overall bone strength caused by iPTH.

Measurements of serum osteocalcin, a marker of bone formation, suggested that iPTH increased bone accretion in T-cell-replete, but not in T-cell-deficient, mice (Figure 1F). Similarly, assessment of the serum levels of C-terminal telopeptide of collagen (CTx), a biochemical marker of resorption, revealed

(C) Measurements of trabecular structural indices by μCT. Trabecular number (Tb.N), trabecular space (Tb.Sp), connectivity density (Conn.D), and structure model index (SMI) are shown.
(D) Ex vivo μCT analysis of femoral cortical bone.
(E) Mechanical testing of the femur by four-point bending tests.
(F) Serum levels of osteocalcin, a marker of formation, and CTx, a marker of resorption.
All data are expressed as mean ± SEM. n = 9–11 mice per group. *$p < 0.05$, **$p < 0.01$, and ***$p < 0.001$ compared to baseline and/or to the corresponding vehicle-treated group. #$p < 0.05$ and ##$p < 0.001$ compared to T-cell-replete, iPTH-treated mice.

Table 1. Effect of iPTH Treatment on Histomorphometric Indices of Trabecular and Cortical Bone Turnover in WT Mice, *TCR*β$^{-/-}$ Mice, and *TCR*β$^{-/-}$ Mice Subjected to Adoptive Transfer of WT T Cells 1 Week before the Initiation of iPTH Treatment

	WT Veh	WT PTH	*TCR*β$^{-/-}$ Veh	*TCR*β$^{-/-}$ PTH	*TCR*β$^{-/-}$ + T Veh	*TCR*β$^{-/-}$ + T PTH
MAR (μm/day)	1.74 ± 0.05	2.06 ± 0.07[a]	1.89 ± 0.07	2.02 ± 0.08	1.75 ± 0.10	2.06 ± 0.09[a]
BFR/BS (μm^3/μm^2/day)	0.62 ± 0.06	1.36 ± 0.05[c]	0.59 ± 0.10	0.88 ± 0.08	0.57 ± 0.06	1.37 ± 0.10[c]
Ob.S (mm)	2.2 ± 0.3	12.0 ± 0.7[c]	2.4 ± 0.2	5.4 ± 0.5[a,d]	2.4 ± 0.2	12.8 ± 0.7[c]
Oc.S (mm)	1.0 ± 0.1	1.7 ± 0.2[a]	0.7 ± 0.1	1.0 ± 0.2	1.0 ± 0.1	1.8 ± 0.2[a]
N.Oc/BS (mm^{-1})	3.1 ± 0.1	1.9 ± 0.3[b]	2.9 ± 0.3	2.5 ± 0.1	3.0 ± 0.3	1.8 ± 0.1[c]
Oc.S/BS (%)	10.1 ± 0.4	6.5 ± 0.9[b]	9.1 ± 0.7	8.0 ± 0.5	9.6 ± 0.9	6.2 ± 0.4[c]
Ec.MAR (μm/day)	2.15 ± 0.2	2.27 ± 0.10	2.10 ± 0.1	2.30 ± 0.20	2.27 ± 0.20	2.33 ± 0.20

Mineral apposition rate (MAR) and bone formation rate (BFR) are dynamic indices of trabecular bone formation. Ob.S (the length of bone surface occupied by osteoblasts) is a static index of trabecular bone formation. Oc.S (the length of bone surface occupied by OCs), N.OC/BS (the number of osteoclasts per mm^2 bone surface), and OcS/BS (the percentage of bone surface occupied by osteoclasts), are indices of trabecular bone resorption. Ec.MAR is an index of endocortical bone formation. n = 9–11 mice per group. All data are expressed as mean ± SEM.
[a] $p < 0.05$ compared to the corresponding vehicle-treated group.
[b] $p < 0.01$ compared to the corresponding vehicle-treated group.
[c] $p < 0.001$ compared to the corresponding vehicle treated group.
[d] $p < 0.05$ compared to T-cell-replete iPTH-treated mice.

that iPTH increased bone resorption in WT mice and in T-cell-reconstituted *TCR*β$^{-/-}$ mice, but not in T-cell-deficient mice. Analysis of the secondary spongiosa by bone histomorphometry confirmed that iPTH increased trabecular bone formation in T-cell-replete mice, but not in *TCR*β$^{-/-}$ mice (Table 1), as assessed by measurements of mineral apposition rate (MAR) and bone formation rate (BFR). In contrast, in all groups, iPTH failed to cause a significant increase in endocortical MAR (Ec.MAR). iPTH had no significant effects on indices of trabecular bone resorption in T-cell-deficient mice, whereas it caused an increase in total OC surface (Oc.S) in WT and T-cell-reconstituted mice. In response to iPTH, T-cell-replete mice also exhibited a decrease in both the number of OCs per bone surface (N.Oc/BS) and the percentage of surfaces covered by OCs (Oc.S/BS), a phenomenon explained by the fact that, in control mice, iPTH increased bone surfaces more markedly than OC number and OC surfaces.

The finding that iPTH fails to stimulate in vivo bone resorption in *TCR*β$^{-/-}$ mice may suggest that iPTH induces T cell production of osteoclastogenic cytokines. Because T cells secrete large amounts of soluble RANKL (Kong et al., 1999), we measured the production of RANKL by BM and spleen CD4+ and CD8+ T cells harvested from WT mice treated with iPTH or vehicle for 4 weeks. These studies revealed that iPTH increased the production of RANKL by BM CD8+ cells by 2- to 3-fold, whereas it had no effects on BM CD4+ cells (Figures S2A and S2B), suggesting that RANKL production by BM CD8+ cells may play a role in the stimulation of bone resorption induced by iPTH. Additional experiments disclosed that iPTH increased by ~30%–~35% the fraction of TNFα+ CD8+ cells and IFNγ+ CD8+ cells (Figure S3A), although this difference was not statistically significant. The stimulation of cytokine production by CD8+ cells caused by PTH was associated with a nonsignificant increase in the expression of the activation marker CD69 and a minimal stimulation of CD25 expression (Figure S3B). iPTH had negligible effects on the expression of both markers on CD4+ cells.

To investigate the effects of iPTH in additional strains of T-cell-deficient mice, iPTH was injected for 4 weeks in nude mice, a strain with a severe deficiency of αβ T cells, and in *Rag2*$^{-/-}$ mice, a strain that lacks both T and B cells. μCT analysis revealed (Figure 2A) that iPTH caused a smaller increase in BV/TV in *Rag2*$^{-/-}$ mice and no increase in BV/TV in nude mice, as compared to WT controls. Measurements of serum osteocalcin showed that iPTH failed to stimulate bone formation in both nude and *Rag2*$^{-/-}$ mice, whereas it caused a significant increase in osteocalcin levels in WT mice. Together, these findings not only confirm that T cells potentiate the anabolic activity of iPTH by stimulating bone formation, but also suggest that, although T cells play an amplificatory role in some strains, in others, the presence of T cells is an essential requirement for iPTH-mediated trabecular bone anabolism.

To characterize the subset of T cells required for iPTH to promote bone anabolism, we injected iPTH in class II *MHC*$^{-/-}$ (*Abb*$^{-/-}$) mice that lack CD4 T cells, class I *MHC*$^{-/-}$ (β2 m$^{-/-}$) mice that lack CD8 T cells, and double *MHC*$^{-/-}$ mice that lack both populations. iPTH markedly increased BV/TV and osteocalcin in WT mice, caused a slightly blunted response in class II *MHC*$^{-/-}$ mice, and induced no changes in class I *MHC*$^{-/-}$ and double *MHC*$^{-/-}$ mice (Figure 2B). These findings suggest that iPTH promotes bone anabolism mostly through CD8+ T cells, and CD4+ cells play a small contributory role.

The pivotal role of CD8+ cells was confirmed by adoptively transferring CD4+ or CD8+ cells into *TCR*β$^{-/-}$ mice. Measurements of BV/TV by μCT revealed (Figure 2C) that iPTH increased BV/TV in WT mice and *TCR*β$^{-/-}$ animals reconstituted with CD8+ T cells, whereas it had no effects in T-cell-deficient mice, *TCR*β$^{-/-}$ mice, and *TCR*β$^{-/-}$ animals reconstituted with CD4+ T cells.

T-Cell-Deficient Mice Exhibit a Blunted Osteoblastogenic Response to iPTH

BM from WT, *TCR*β$^{-/-}$, and T-cell-reconstituted *TCR*β$^{-/-}$ mice treated with iPTH was utilized to assess the formation of alkaline phosphatase (ALP)-positive colony-forming unit fibroblast (CFU-F), herein defined CFU-ALP, an index of SC commitment to the osteoblastic lineage. iPTH treatment increased by ~2-fold the CFU-ALP formation in the BM of T-cell-replete mice, whereas it had no effect in that of *TCR*β$^{-/-}$ mice (Figure 3A), thus

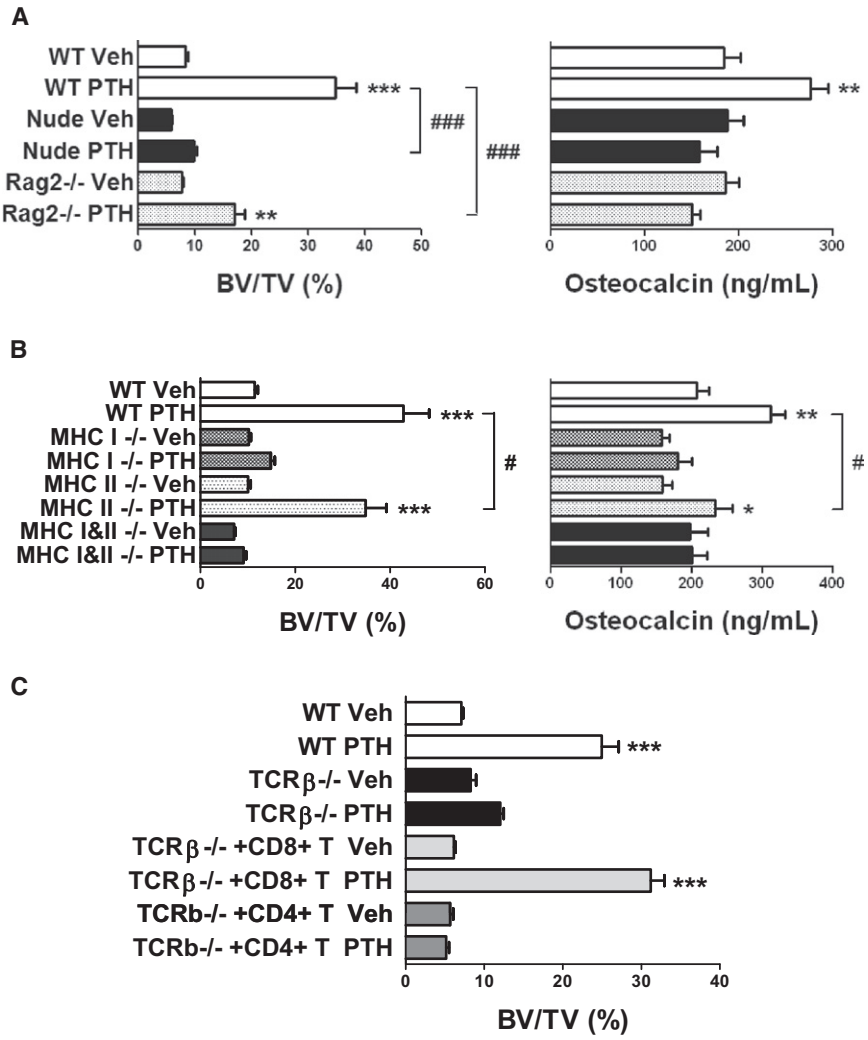

Figure 2. Analysis of the Effects of iPTH Treatment in Additional Strains of T-Cell-Deficient Mice

(A) Trabecular BV/TV and serum osteocalcin levels in nude and *RAG2*$^{-/-}$ mice. n = 11–13 mice per group.

(B) Trabecular BV/TV and serum osteocalcin levels in class II *MHC*$^{-/-}$ mice that lack CD4 T cells, class I *MHC*$^{-/-}$ mice that lack CD8 T cells, and double *MHC*$^{-/-}$ mice that lack both populations. n = 6–8 mice per group.

(C) Trabecular BV/TV in *TCR*β$^{-/-}$ mice subjected to adoptive transfer of either CD4+ or CD8+ T cells 1 week before initiation of iPTH. n = 5–10 mice per group.

All data are expressed as mean ± SEM. ***$p < 0.001$ compared to the corresponding vehicle treated group. *$p < 0.05$, **$p < 0.01$, ***$p < 0.001$ compared to the corresponding vehicle-treated group. #$p < 0.05$ and ###$p < 0.001$ compared to the indicated groups.

indicating that T cells potentiate the capacity of iPTH to increase the number of SCs with osteogenic potential.

To directly evaluate the role of T cells in iPTH-induced osteoblastogenesis, we cultured BM from iPTH-treated T-cell-replete and *TCR*β$^{-/-}$ mice for 1 week to allow SCs to proliferate and differentiate into pre-OBs. Pre-OBs were then purified and counted. This analysis revealed (Figure 3B) that in vivo iPTH treatment increases the number of pre-OBs by ~50% in samples from WT and T-cell-reconstituted *TCR*β$^{-/-}$ mice. In contrast, iPTH had no effects on the number of pre-OBs from *TCR*β$^{-/-}$ mice. To investigate the mechanism involved, BM was cultured for 1 week, and pre-OBs were purified and used to determine their rate of proliferation and apoptosis. These experiments revealed that iPTH increases significantly the proliferation of WT and T-cell-reconstituted *TCR*β$^{-/-}$ mice pre-OBs, but not those from *TCR*β$^{-/-}$ mice (Figure 3C). Moreover, iPTH decreased the rate of pre-OB apoptosis in all groups of mice. However, the antiapoptotic effect of iPTH was smaller in pre-OBs from *TCR*β$^{-/-}$ mice than in those from WT and T-cell-reconstituted *TCR*β$^{-/-}$ controls (Figure 3D). Analysis of the expression levels of osteoblastic genes in pre-OBs revealed that iPTH increases the expression of type 1 collagen mRNA by ~5-fold and that of Runx2, Osterix, Bone Sialoprotein, and Osteocalcin mRNAs by ~2-fold in pre-OBs from WT mice and T-cell-reconstituted *TCR*β$^{-/-}$ mice (Figure 3E). In contrast, iPTH had no effects on the expression of OB-related genes in cells from *TCR*β$^{-/-}$ mice, thus demonstrating that T cells promote the capacity of iPTH to expand the osteoblastic pool and cell differentiation along the osteoblastic lineage.

T Cells Regulate Osteoblastogenesis through Wnt10b

To determine whether T cells are required for iPTH to activate Wnt signaling in osteoblastic cells, we cultured BM from iPTH-treated WT and *TCR*β$^{-/-}$ mice for 1 week and purified pre-OBs. Pre-OB expression of mRNA for genes known to be upregulated by Wnt signaling was then assessed by real-time RT-PCR. The analyzed genes were chosen based on known expression patterns during differentiation of primitive mesenchymal cells to the osteoblast phenotype. Some of the selected genes are known to play a direct role in regulating OB differentiation (Vaes et al., 2005), whereas others are not involved in OB differentiation but are sensitive markers of Wnt activation (Jackson et al., 2005). These analyses revealed (Figure 4A) that iPTH activates Wnt signaling in pre-OBs through T cells, as pre-OB levels of mRNA for 9 of the 12 tested genes were all increased by iPTH in pre-OBs from WT, but not in those from T-cell-deficient *TCR*β$^{-/-}$ mice, whereas the mRNA levels of the remaining three genes were not increased by iPTH in both WT and *TCR*β$^{-/-}$ mice. The nine genes that were stimulated by iPTH were: aryl-hydrocarbon receptor (*Ahr*), axin2, cysteine-rich protein 61 (*Cyr61*), naked cuticle 2 homolog (*Nkd2*), transgelin (*tagln*), transforming growth factor β3 (*TGFβ3*), thrombospondin 1 (*Thbs1*), twist gene homolog 1 (*Twst1*), and Wnt1-inducible signaling pathway protein 1 (*Wisp1*). The three genes that were not stimulated by iPTH were: cyclin D1 (*Ccnd1*), insulin-like

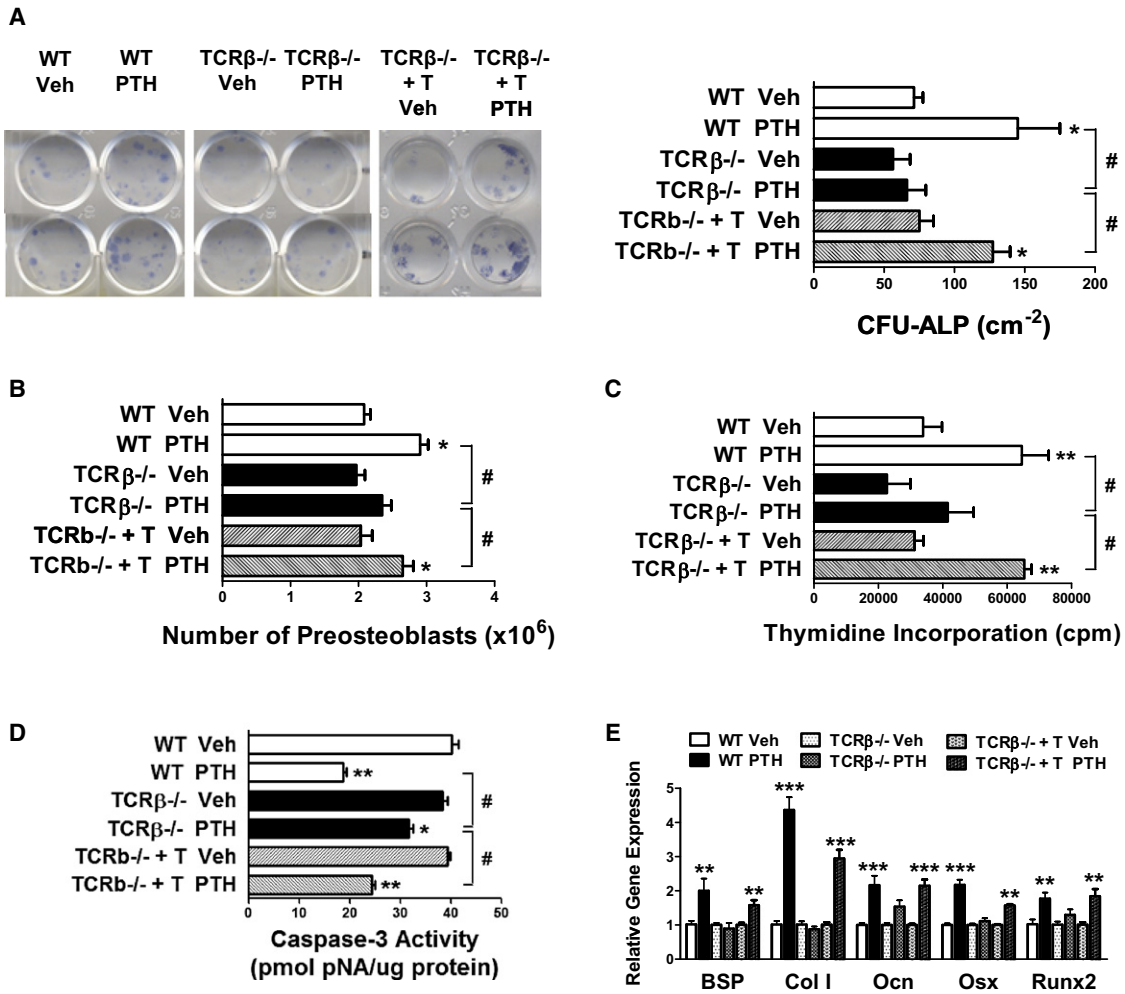

Figure 3. Analysis of the Effects of iPTH Treatment on Osteoblastogenesis and Pre-OB Apoptosis in WT, *TCR*β$^{-/-}$ Mice, and *TCR*β$^{-/-}$ Mice Previously Subjected to Adoptive Transfer of WT T Cells

(A) Whole BM was cultured for 7 days to assess the formation CFU-ALP. (Left) Representative duplicate wells per group. (Right) The average of the colonies counted in 6 wells.

(B) BM harvested at sacrifice was cultured for 1 week, and pre-OBs were purified and counted.

(C) Pre-OBs were purified from BM cultured for 1 week, seeded in equal number, and pulsed with [^{3}H]-thymidine for 18 hr to assess their proliferation. Data are expressed in CPM.

(D) Pre-OBs were purified from BM cultured for 1 week, and the rate of apoptosis was quantified by determinations of caspase 3 activity.

(E) Pre-OBs were purified from BM cultured for 1 week, and the levels of OB marker gene mRNAs, bone sialoprotein (BSP), type I collagen (Col1a1), osteocalcin (Ocn), osterix (Osx), and runt-related transcription factor 2 (Runx2) were analyzed by RT-PCR.

All data are expressed as mean ± SEM. n = 4–5 per group. *$p < 0.05$, **$p < 0.01$, and ***$p < 0.001$ compared to the corresponding vehicle-treated group. #$p < 0.001$ compared to the indicated group.

growth factor binding protein 2 (*Igfbp2*), and osteomodulin (*Omd*).

Having established that T cells are required for iPTH to activate Wnt signaling in OBs, we sought to identify the ligands involved. Wnt10b is a candidate factor produced by mesenchymal stem cells and T lymphocytes (Hardiman et al., 1996; Ouji et al., 2006), which promotes OB differentiation and increases bone density (Bennett et al., 2005). To determine whether iPTH increases Wnt10b expression and the responsible cell lineages, BM was harvested from WT and *TCR*β$^{-/-}$ mice treated with iPTH or vehicle for 4 weeks and assayed for Wnt10b mRNA levels. BM from WT mice was also utilized to purify pre-OBs, dendritic cells (DCs), T cells, monocytes, and B cells. Analysis by real-time RT-PCR disclosed that iPTH increases the whole BM expression of Wnt10b mRNA by 2-fold in WT mice, but not in *TCR*β$^{-/-}$ mice. Among individual lineages of WT BM, T lymphocytes were the only cells that responded to iPTH with a significant increase (~5-fold) in Wnt10b expression (Figure 4B).

To characterize the PTH-responsive T cell subset, CD4+ and CD8+ cells were purified from the spleen and the BM of iPTH-treated WT mice and analyzed by real-time RT-PCR. These studies disclosed that iPTH treatment increases the levels of Wnt10b mRNA in BM CD4+ and CD8+ T cells by ~4-fold and ~13-fold, respectively (Figure 4C). In contrast, iPTH had no

effects on Wnt10b mRNA levels in spleen CD4+ and CD8+ T cells. Analysis of Wnt7a and Wnt3a, two ligands that also promote bone anabolism, disclosed that iPTH caused a ~4-fold increase in CD4+ cell production of Wnt7b mRNA but failed to alter the mRNA levels of Wnt3a in all populations of T cells. Further analysis by western blotting confirmed that iPTH upregulates the production of Wnt10b by BM CD8+ T cells by ~4.5-fold (Figure 4D). In contrast, Wnt7b protein was not detected in spleen and BM CD4+ and CD8+ T cells (Figure S4A), indicating that T-cell-produced Wnt7b does not contribute to activate Wnt signaling in OBs.

To determine whether T-cell-produced Wnt10b has the capacity to activate canonical Wnt signaling in OBs, CD4+ and CD8+ T cells purified from the BM of iPTH-treated WT mice were cocultured with the osteoblastic cell line MC3T3-E1 and transiently transfected with the β-catenin/TCF-luciferase reporter plasmid TOPFLASH or with the negative control plasmid FOPFLASH (Almeida et al., 2005). Analysis of luciferase activity in transfected MC3T3-E1 cells revealed that, whereas the addition of CD8+ T cells from iPTH-treated mice activates TCF-mediated transcription, the addition of CD4+ T cells does not (Figure 4E). Together, these findings demonstrate that iPTH upregulates the CD8+ T cell production of Wnt10b and that T-cell-produced Wnt10b activates canonical Wnt signaling in osteoblastic cells.

WT and *Wnt10b*$^{-/-}$ donor mice were similar with respect to CD4+/CD8+ ratio (Figure S5A) and numbers of naive and memory BM T cells (Figure S5B). Furthermore, WT and *Wnt10b*$^{-/-}$ T cells exhibit similar rates of proliferation (Figure S5C) and expression of activation markers in response to T cell receptor crosslinking (Figure S5D). However, mice lacking *Wnt10b*$^{-/-}$ have a markedly decreased bone volume and bone formation (Bennett et al., 2005), a phenotype that prevents establishing the role of Wnt10b in PTH-induced bone anabolism by comparing the response of WT and *Wnt10b*$^{-/-}$ mice to iPTH. Therefore, to demonstrate the specific relevance of T-cell-produced Wnt10b in vivo, equal numbers of splenic T cells from WT and *Wnt10b*$^{-/-}$ mice were adoptively transferred into 6-week-old *TCR*β$^{-/-}$ mice. After 1 week, reconstituted mice were treated with vehicle or iPTH for 4 weeks. FACS analysis of splenocytes harvested at sacrifice from mice subjected to adoptive transfer of T cells revealed that mice reconstituted with WT T cells and *Wnt10b*$^{-/-}$ T cells had similar numbers of CD4+ and CD8+ cells (Figure S6).

Measurements of femoral BV/TV by μCT and of serum indices of turnover at 4 weeks revealed (Figure 4G) that iPTH increased BV/TV and osteocalcin in WT mice and in *TCR*β$^{-/-}$ animals reconstituted with WT T cells, whereas it had no effects in both T-cell-deficient mice and *TCR*β$^{-/-}$ mice reconstituted with *Wnt10b*$^{-/-}$ T cells. In contrast, iPTH failed to augment CTx levels in T-cell-deficient mice but increased CTx levels in *TCR*β$^{-/-}$ mice reconstituted with WT or *Wnt10b*$^{-/-}$ T cells. These findings demonstrate that iPTH stimulates bone formation and promotes bone anabolism through T-cell-produced Wnt10b.

In Vitro PTH Treatment Stimulates T Cell Wnt10b Production

To investigate whether T cells have the capacity to directly respond to PTH, 99% pure splenic CD4+ and CD8+ T cells were prepared from untreated WT mice by immunomagnetic cell sorting (Figure S7). The PTH receptor PPR was found to be expressed in both CD4+ and CD8+ cells, although the levels of the receptor were higher in CD8+ cells (Figure 5A). Stimulation of T cells by PTH induced a significant increase in the production of cAMP in both CD4+ and CD8+ cells within 10 min (Figure 5B), demonstrating that both T cell lineages are responsive to PTH. In vitro treatment with PTH for 3 hr increased the expression of Wnt10b mRNA by nonactivated CD8+ T cells cultured with and without the phosphodiesterase inhibitor 3-isobutyl-1-methylxanthine (IBMX) (Figure 5C), although the stimulatory effect of PTH was significantly higher in IBMX pretreated cells. PTH did not induce a higher expression of Wnt10b in activated CD8+ cells, indicating that T cell activation is not required for PTH induction of Wnt10b production. Pretreatment with H89, a specific PKA inhibitor, abolished PTH increase in Wnt10b mRNA expression in resting CD8+ T cells (Figure 5D), suggesting that PTH increases Wnt10b mRNA expression primarily through the Gs/cAMP/PKA pathway. PTH also increased Wnt10b mRNA production by IBMX-treated human CD8+ T cells (Figure 5E), though it did not alter Wnt10b mRNA levels in murine pre OBs (Figure 5F). These findings demonstrate that PTH has the capacity to directly stimulate T cell production of Wnt10b in vitro.

DISCUSSION

We report that iPTH markedly increases the production of Wnt10b by bone marrow CD8+ T cells and that the activation of Wnt signaling in osteoblastic cells by T-cell-produced Wnt10b plays a relevant role in the mechanism by which iPTH increases bone strength. This insight supports a role for immune cell-bone cell crosstalk in the mechanism of action of PTH.

T cells were found to augment the capacity of iPTH to improve architecture in trabecular, but not in cortical, bone. Although the reason of this selectivity is unknown, a lack of access of T cells to cortical surfaces is not a likely explanation, as T cells reach endosteal and periosteal bone surface through blood vessels and recirculate in and out of the BM (Di Rosa, 2008).

The relevance of T cells in vivo was demonstrated in *TCR*β$^{-/-}$ mice and confirmed in additional T-cell-deficient strains *RAG2*$^{-/-}$, nude, and *MHC*$^{-/-}$ mice. Our findings extend earlier observations by Pettway et al., who reported that daily injections of PTH for up to 7 weeks did not induce vertebral bone growth in nude mice (Pettway et al., 2005). In *MHC*$^{-/-}$ and nude mice, the anabolic activity of iPTH was completely absent, whereas in the others, it was markedly, but not completely, silenced. Moreover, in *TCR*β$^{-/-}$ mice, the anabolic activity of iPTH was more attenuated in animals treated from 7 to 11 weeks of age than in those started on iPTH at 5 weeks.

Osteoblastic cells produce several bone anabolic Wnt ligands, including Wnt10b, Wnt7a, and Wnt3b (Luo et al., 2004; Rawadi et al., 2003). These factors are likely to contribute to the T-cell-independent anabolic activity of iPTH, and quantitative differences in their production may account, in part, to the strain and age-dependent variability in the response to iPTH observed herein. Furthermore, the magnitude of the anabolic response to iPTH in T cell null mice may be related to a strain- and age-dependent capacity of iPTH to inhibit the bone cells' production of Wnt inhibitors such as sclerostin (Bellido et al., 2005; Keller

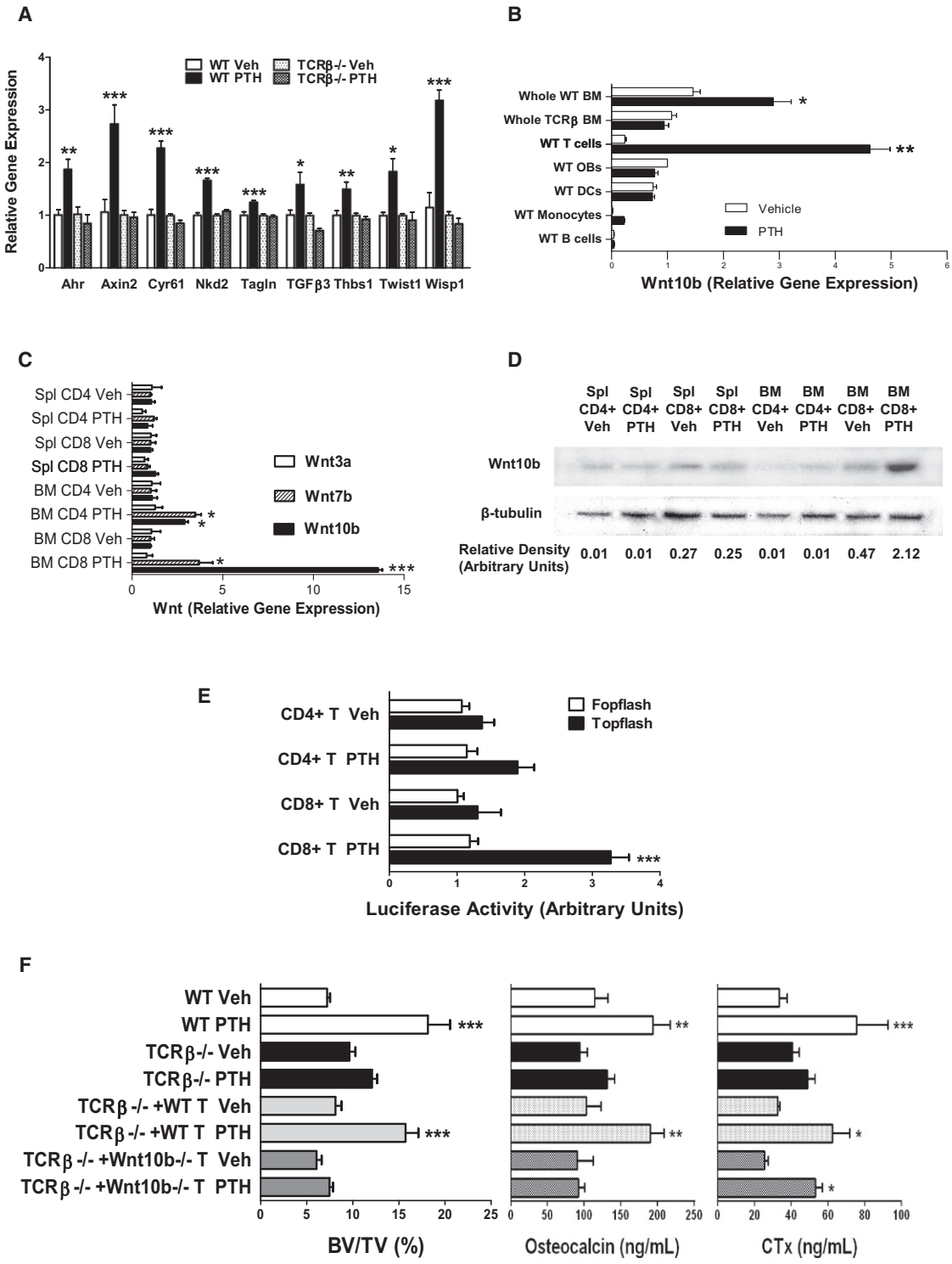

Figure 4. Analysis of the Role of Wnt10b and Wnt Signaling in iPTH-Induced Anabolism

(A) Effect (mean ± SEM) of iPTH on the expression of mRNA of genes known to be upregulated by Wnt signaling, aryl-hydrocarbon receptor (*Ahr*), axin2, cysteine-rich protein 61 (*Cyr61*), naked cuticle 2 homolog (*Nkd2*), transgelin (*tagln*), transforming growth factor β 3 (*TGFβ3*), thrombospondin 1 (*Thbs1*), twist gene homolog 1 (*Twst1*), and Wnt1-inducible signaling pathway protein 1 (Wisp1). BM was harvested at sacrifice from WT and *TCRβ*$^{-/-}$ treated with vehicle of iPTH. BM was cultured for 1 week, pre-OBs were purified, and mRNA levels were determined by RT-PCR. n = 4 mice per group.

(B) Effect (mean ± SEM) of iPTH on the expression of Wnt10b mRNA in whole BM and BM T cells, dendritic cells, monocytes, B cells, and pre-OBs purified from BM samples obtained at sacrifice. Data are expressed relative to pre-OBs from vehicle treated mice. n = 10 mice per group.

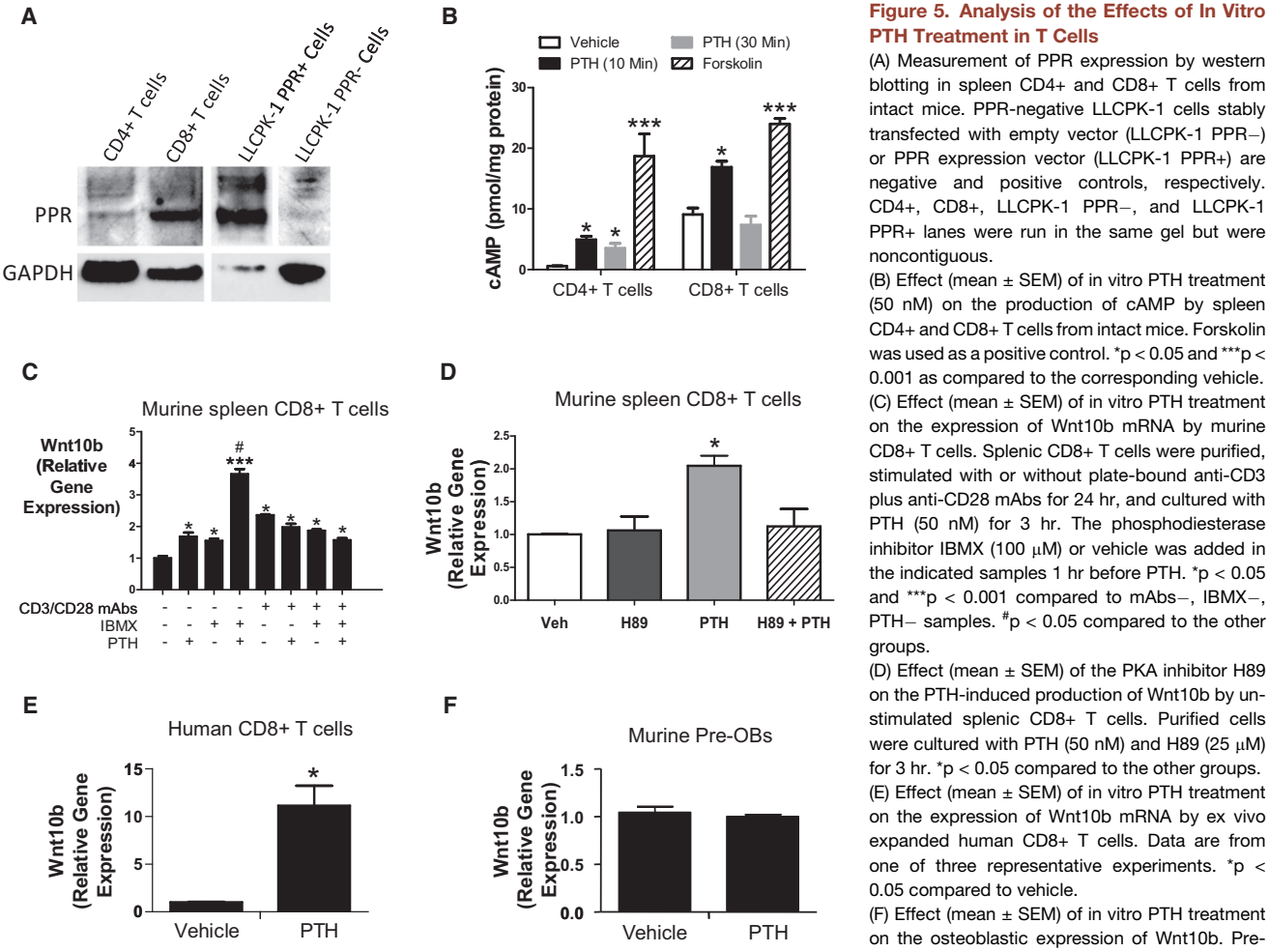

Figure 5. Analysis of the Effects of In Vitro PTH Treatment in T Cells

(A) Measurement of PPR expression by western blotting in spleen CD4+ and CD8+ T cells from intact mice. PPR-negative LLCPK-1 cells stably transfected with empty vector (LLCPK-1 PPR–) or PPR expression vector (LLCPK-1 PPR+) are negative and positive controls, respectively. CD4+, CD8+, LLCPK-1 PPR–, and LLCPK-1 PPR+ lanes were run in the same gel but were noncontiguous.

(B) Effect (mean ± SEM) of in vitro PTH treatment (50 nM) on the production of cAMP by spleen CD4+ and CD8+ T cells from intact mice. Forskolin was used as a positive control. *$p < 0.05$ and ***$p < 0.001$ as compared to the corresponding vehicle.

(C) Effect (mean ± SEM) of in vitro PTH treatment on the expression of Wnt10b mRNA by murine CD8+ T cells. Splenic CD8+ T cells were purified, stimulated with or without plate-bound anti-CD3 plus anti-CD28 mAbs for 24 hr, and cultured with PTH (50 nM) for 3 hr. The phosphodiesterase inhibitor IBMX (100 μM) or vehicle was added in the indicated samples 1 hr before PTH. *$p < 0.05$ and ***$p < 0.001$ compared to mAbs–, IBMX–, PTH– samples. #$p < 0.05$ compared to the other groups.

(D) Effect (mean ± SEM) of the PKA inhibitor H89 on the PTH-induced production of Wnt10b by unstimulated splenic CD8+ T cells. Purified cells were cultured with PTH (50 nM) and H89 (25 μM) for 3 hr. *$p < 0.05$ compared to the other groups.

(E) Effect (mean ± SEM) of in vitro PTH treatment on the expression of Wnt10b mRNA by ex vivo expanded human CD8+ T cells. Data are from one of three representative experiments. *$p < 0.05$ compared to vehicle.

(F) Effect (mean ± SEM) of in vitro PTH treatment on the osteoblastic expression of Wnt10b. Pre-OBs were purified from the BM of untreated WT mice and were cultured with PTH 50 nM for 3 hr.

and Kneissel, 2005), Dickkopf-1 (Kulkarni et al., 2005), and Sfrp-4 (Qin et al., 2003). These factors have been shown to contribute to the anabolic activity of iPTH through T-cell-independent mechanisms. Because B cells are regulated by PTH (Alexiewicz et al., 1990), the response of *RAG2*$^{-/-}$ mice to iPTH might also have been determined by the lack of B cells, which is a feature of *RAG2*$^{-/-}$ mice.

The enhancement of bone formation induced by iPTH is accompanied by a stimulation of bone resorption, which is driven by increased production of RANKL and decreased release of OPG in the bone microenvironment (Ma et al., 2001). The direct effects of PTH on RANKL/OPG production are mitigated, in part, by the iPTH-induced activation of β catenin in OBs, as this transcriptional regulator stimulates their production of OPG (Glass et al., 2005) and represses that of RANKL (Spencer et al., 2006). The latter is one of the mechanisms that prevent bone resorption from offsetting the anabolic activity of iPTH. Accordingly, we found that iPTH increased CTx levels and total OC surfaces in T-cell-replete mice. In agreement with studies by others (Iida-Klein et al., 2002), the stimulation of bone resorption induced by iPTH was not reflected by measurements of the number of OCs and OC surfaces per unit of trabecular bone

(C) Effect (mean ± SEM) of iPTH on the expression of Wnt3a, Wnt7b, and Wnt10b mRNA in spleen and BM CD4+ and CD8+ T cells purified from samples harvested at sacrifice. n = 10 mice per group.

(D) Measurement of Wnt10b protein levels by western blotting in spleen and BM CD4+ and CD8+ T cells purified from samples harvested at sacrifice. The bottom panel shows the densitometric quantification of the data shown in the top panel. n = 10 mice per group.

(E) Effect (mean ± SEM) of T cells from iPTH-treated mice on Wnt signaling in the MC3T3-E1 osteoblastic cell line. MC3T3-E1 cells were transiently transfected with the TCF-luciferase reporter (TOPFLASH) or a control vector lacking the TCF-binding site (FOPFLASH) and were cocultured with either CD4+ or CD8+ T cells derived from the BM of WT mice treated with iPTH. Data are expressed as the mean of triplicate determinations of luciferase activity normalized for pRL-TK activity. n = 4 mice per group.

(F) Analysis of the effects (mean ± SEM) of iPTH treatment in WT mice, *TCR*β$^{-/-}$ mice, and *TCR*β$^{-/-}$ mice subjected to adoptive transfer of T cells derived from WT mice and *Wnt10b*$^{-/-}$ mice 1 week before initiation of iPTH. The panels show trabecular BV/TV as measured by μCT at sacrifice and serum osteocalcin and CTx at 4 weeks. n = 8 mice per group. *$p < 0.05$, **$p < 0.01$, and *** = $p < 0.001$ compared to the corresponding vehicle-treated group.

surface. This was mainly because, in control mice, iPTH increased bone surfaces more markedly than OC number and OC surfaces. As a result, the percentages of OC surfaces were observed to be slightly decreased. By contrast, neither CTx nor histomorphometric indices of bone resorption was significantly affected by iPTH in T-cell-deficient mice. In a previous study, continuous PTH treatment was similarly found unable to stimulate bone resorption in T-cell-depleted mice (Gao et al., 2008). The capacity of iPTH to elicit a resorptive response in T-cell-replete mice, but not in T-cell-deficient animals, may be explained, in part, by the increased production of RANKL by BM CD8+ T cells induced by iPTH. Another likely contributory mechanism is the capacity of T cells to lead to the generation of BM SCs, which respond to PTH by producing higher levels of RANKL and lower levels of OPG, as compared to the SCs that differentiate in the BM of T-cell-deficient mice (Gao et al., 2008).

We show herein that osteoblastic cells from WT mice treated with iPTH in vivo exhibited increased commitment to the osteoblastic lineage, proliferation, differentiation, and life span in vitro, as compared to the corresponding cells from T-cell-deficient mice. Thus, T cells, like PTH, affect all aspects of OB life cycle. Remarkably, these differences were demonstrated in OBs purified from BM cultured for 7 days without the addition of PTH, suggesting that, in vivo, the hormone regulates early commitment steps of SCs and their osteoblastic progeny through T-cell-produced Wnt10b and that these steps are not reversed by the absence of PTH and T cells in vitro. This model is consistent with the capacity of Wnt signaling to guide cell fate determination (Moon et al., 2002). A similar paradigm has been described in ovariectomized mice, a model in which estrogen withdrawal in vivo leads to the formation of SCs, which exhibit an increased osteoclastogenic activity that persists in vitro for 4 weeks (Kimble et al., 1996).

Activation of the Wnt-signaling pathway in cells of the osteoblastic lineage plays a relevant role in iPTH-induced anabolism (Bodine and Komm, 2006; Kulkarni et al., 2005), but the specific signaling molecules involved remains uncertain. LRP5 is now recognized to stimulate bone formation by inhibiting serotonin synthesis in the duodenum, rather than functioning as a Wnt coreceptor in OBs (Yadav et al., 2008). Accordingly, *LRP5*$^{-/-}$ mice are fully responsive to iPTH (Iwaniec et al., 2007; Sawakami et al., 2006). iPTH may promote Wnt signaling by activating the closely related receptor LRP6, which is also expressed in cells of the osteoblastic lineage (Jilka, 2007). Alternatively, iPTH could activate noncanonical Wnt-signaling pathways that are independent of LRP5 and LRP6. Our data show that T cells activate canonical Wnt signaling in pre-OBs. However, we have not determined whether T cells activate LRP5 or LRP6 signaling in pre-OBs nor the effects of T cells on noncanonical Wnt signaling.

The specific Wnt ligands responsible for the iPTH-induced activation of Wnt signaling are also unknown. We found that iPTH markedly upregulates the production of Wnt10b by BM CD8+ T cells and that the capacity of activating Wnt signaling in an osteoblastic line is a feature of CD8+ T cells. The relevance of CD8+ cells was demonstrated by the inability of iPTH to promote bone anabolism in class I *MHC*$^{-/-}$ mice, and the pivotal role of T-cell-produced Wnt10b was revealed by the hampered effect of iPTH on BV/TV and bone turnover in *TCR*$\beta^{-/-}$ mice reconstituted with T cells from *Wnt10b*$^{-/-}$ mice. iPTH also caused a small increase in the production of Wnt10b by BM CD4+ cells, which was associated with a slightly diminished anabolic response in class II *MHC*$^{-/-}$ mice, suggesting that production of Wnt10b by CD4+ cells contributes, in small part, to the anabolic activity of iPTH.

It is likely that iPTH directly targets CD8+ T cells and stimulates their production of Wnt10b. This hypothesis is supported by the strong expression of PPR in CD8+ T cells and the capacity of in vitro PTH treatment to promote cAMP production and Wnt10b expression in CD8+ murine and human lymphocytes. However, we cannot conclusively exclude that in vivo iPTH treatment might induce CD8+ T cell production of Wnt10b indirectly.

Whereas in vitro PTH treatment increased Wnt10b mRNA expression in splenic T cells, iPTH upregulated Wnt10b production only by BM T cells. This diversity might be explained by the different dose and time of exposure to PTH. However, because adoptive transfer of spleen T cells into *TCR*$\beta^{-/-}$ mice was followed by a restoration of a full responsiveness to iPTH, the data suggest that the capacity of T cells to upregulate their production of Wnt10b in response to iPTH is not an intrinsic feature of T cells, but rather is induced by environmental cues.

In summary, this study indicates that T cells represent a regulatory component of the BM microenvironment involved in the anabolic response to iPTH. Bone anabolism is induced by PPR signaling in SCs and their osteoblastic progeny, but T cells play a permissive role by producing Wnt10b in response to stimulation by iPTH. Understanding the crosstalk between T cells and osteoblastic cells may thus yield novel therapeutic strategies for potentiating bone anabolic agents.

EXPERIMENTAL PROCEDURES

Animals

The animal procedures were approved by the Institutional Animal Care and Use Committee of Emory University. Additional information is provided in the Supplemental Data.

Intermittent Administration of PTH

Human PTH (1–34) (Bachem California, Inc., Torrance, CA) or vehicle were injected at doses of 80 μg/kg/day subcutaneously for 4 weeks in 5- to 6-week-old mice.

Purification of T and B Cells, Monocytes, and Dendritic Cells and T Cell Transfer

Information is provided in the Supplemental Data.

Flow Cytometry

Splenocytes and BM cells were stained with APC anti-mouse CD4 (BioLegend, San Diego, CA), PerCP anti-mouse CD8, FITC anti-mouse MHCII, PE anti-mouse CD20, PE anti-mouse Cd11b, PE anti-mouse CD69, and FITC anti-mouse CD25 (BD Biosciences, San Jose, CA) mAbs and propidium Iodide solution. Samples were analyzed by flow cytometry on a FACSort flow cytometer (BD Biosciences).

In Vivo BMD Measurements

Total body and femoral BMD were measured in anesthetized mice using a PIXImus2 bone densitometer (GE Medical System, Lunar, Madison, WI) as described (Cenci et al., 2003).

μCT Measurements

μCT scanning and analysis was performed as reported previously (Gao et al., 2007), using a Scanco μCT-40 scanner (Scanco Medical, Bassersdorf, Switzerland). Cortical bone volume and cortical thickness were determined by analyzing 80 slices at the middiaphysis of the femurs.

Bone Histology and Quantitative Bone Histomorphometry

Histology of the distal metaphysis of the left femora was performed by the Histomorphometry and Molecular Analysis Core Laboratory of the Center for Metabolic Bone Disease, University of Alabama at Birmingham as described (Gao et al., 2008). Additional information is provided in the Supplemental Data.

Mechanical Testing

The mechanical properties of the right femora were analyzed via four-point bending as described elsewhere (Robertson et al., 2006). Each femur was tested to failure at a displacement rate of 0.05 mm/s, with the supports centered on the middiaphysis and the anterior side of the bone in tension. The resultant force displacement curves were analyzed to obtain force and deflection data.

Markers of Bone Turnover

Serum osteocalcin was measured using Rat-MID Osteocalcin ELISA kit (Immunodiagnostic Systems Inc., Fountain Hills, AZ). Serum CTx was measured using the RatLaps ELISA kit (Immunodiagnostic Systems Inc., Fountain Hills, AZ).

CFU-ALP Assay

Colony-forming assays were carried out as described (Gao et al., 2008). Real-time RT-PCR, thymidine incorporation assay, apoptosis assay, luciferase assay, cAMP assay, western blots, and statistical analysis information are provided in the Supplemental Data.

SUPPLEMENTAL DATA

Supplemental Data include Supplemental Experimental Procedures and eight figures and can be found with this article online at http://www.cell.com/cell-metabolism/supplemental/S1550-4131(09)00228-9.

ACKNOWLEDGMENTS

This study was supported by grants from the National Institutes of Health (AR54625 and AG28278). We are grateful to Laurie McCauley (University of Michigan) for her review of the manuscript.

Received: March 18, 2009
Revised: June 22, 2009
Accepted: July 14, 2009
Published: September 1, 2009

REFERENCES

Alexiewicz, J.M., Klinger, M., Pitts, T.O., Gaciong, Z., Linker-Israeli, M., and Massry, S.G. (1990). Parathyroid hormone inhibits B cell proliferation: implications in chronic renal failure. J. Am. Soc. Nephrol. *1*, 236–244.

Almeida, M., Han, L., Bellido, T., Manolagas, S.C., and Kousteni, S. (2005). Wnt proteins prevent apoptosis of both uncommitted osteoblast progenitors and differentiated osteoblasts by beta-catenin-dependent and -independent signaling cascades involving Src/ERK and phosphatidylinositol 3-kinase/AKT. J. Biol. Chem. *280*, 41342–41351.

Behrens, J., von Kries, J.P., Kuhl, M., Bruhn, L., Wedlich, D., Grosschedl, R., and Birchmeier, W. (1996). Functional interaction of beta-catenin with the transcription factor LEF-1. Nature *382*, 638–642.

Bellido, T., Ali, A.A., Plotkin, L.I., Fu, Q., Gubrij, I., Roberson, P.K., Weinstein, R.S., O'Brien, C.A., Manolagas, S.C., and Jilka, R.L. (2003). Proteasomal degradation of Runx2 shortens parathyroid hormone-induced anti-apoptotic signaling in osteoblasts. A putative explanation for why intermittent administration is needed for bone anabolism. J. Biol. Chem. *278*, 50259–50272.

Bellido, T., Ali, A.A., Gubrij, I., Plotkin, L.I., Fu, Q., O'Brien, C.A., Manolagas, S.C., and Jilka, R.L. (2005). Chronic elevation of parathyroid hormone in mice reduces expression of sclerostin by osteocytes: a novel mechanism for hormonal control of osteoblastogenesis. Endocrinology *146*, 4577–4583.

Bennett, C.N., Longo, K.A., Wright, W.S., Suva, L.J., Lane, T.F., Hankenson, K.D., and MacDougald, O.A. (2005). Regulation of osteoblastogenesis and bone mass by Wnt10b. Proc. Natl. Acad. Sci. USA *102*, 3324–3329.

Bodine, P.V., and Komm, B.S. (2006). Wnt signaling and osteoblastogenesis. Rev. Endocr. Metab. Disord. *7*, 33–39.

Bodine, P.V., Billiard, J., Moran, R.A., Ponce-de-Leon, H., McLarney, S., Mangine, A., Scrimo, M.J., Bhat, R.A., Stauffer, B., Green, J., et al. (2005). The Wnt antagonist secreted frizzled-related protein-1 controls osteoblast and osteocyte apoptosis. J. Cell. Biochem. *96*, 1212–1230.

Calvi, L.M., Sims, N.A., Hunzelman, J.L., Knight, M.C., Giovannetti, A., Saxton, J.M., Kronenberg, H.M., Baron, R., and Schipani, E. (2001). Activated parathyroid hormone/parathyroid hormone-related protein receptor in osteoblastic cells differentially affects cortical and trabecular bone. J. Clin. Invest. *107*, 277–286.

Cenci, S., Toraldo, G., Weitzmann, M.N., Roggia, C., Gao, Y., Qian, W.P., Sierra, O., and Pacifici, R. (2003). Estrogen deficiency induces bone loss by increasing T cell proliferation and lifespan through IFN-gamma-induced class II transactivator. Proc. Natl. Acad. Sci. USA *100*, 10405–10410.

Di Rosa, F. (2008). T-lymphocyte interaction with stromal, bone and hematopoietic cells in the bone marrow. Immunol. Cell Biol. *87*, 20–29.

Dobnig, H., and Turner, R.T. (1995). Evidence that intermittent treatment with parathyroid hormone increases bone formation in adult rats by activation of bone lining cells. Endocrinology *136*, 3632–3638.

Gao, Y., Grassi, F., Ryan, M.R., Terauchi, M., Page, K., Yang, X., Weitzmann, M.N., and Pacifici, R. (2007). IFN-gamma stimulates osteoclast formation and bone loss in vivo via antigen-driven T cell activation. J. Clin. Invest. *117*, 122–132.

Gao, Y., Wu, X., Terauchi, M., Li, J.Y., Grassi, F., Galley, S., Yang, X., Weitzmann, M.N., and Pacifici, R. (2008). T cells potentiate PTH-induced cortical bone loss through CD40L signaling. Cell Metab. *8*, 132–145.

Geffner, M.E., Bersch, N., Cortez, A.B., Bailey, R.C., and Golde, D.W. (1995). Growth-promoting actions of parathyroid hormone, adrenocorticotrophic hormone, and thyroid-stimulating hormone: in vitro studies in normal and pygmy T-lymphoblast cell lines. Pediatr. Res. *37*, 507–511.

Gensure, R.C., Gardella, T.J., and Juppner, H. (2005). Parathyroid hormone and parathyroid hormone-related peptide, and their receptors. Biochem. Biophys. Res. Commun. *328*, 666–678.

Glass, D.A., II, Bialek, P., Ahn, J.D., Starbuck, M., Patel, M.S., Clevers, H., Taketo, M.M., Long, F., McMahon, A.P., Lang, R.A., and Karsenty, G. (2005). Canonical Wnt signaling in differentiated osteoblasts controls osteoclast differentiation. Dev. Cell *8*, 751–764.

Grey, A.B., Stapleton, J.P., Evans, M.C., and Reid, I.R. (1996). Accelerated bone loss in post-menopausal women with mild primary hyperparathyroidism. Clin. Endocrinol. (Oxf.) *44*, 697–702.

Hardiman, G., Albright, S., Tsunoda, J., McClanahan, T., and Lee, F. (1996). The mouse Wnt-10B gene isolated from helper T cells is widely expressed and a possible oncogene in BR6 mouse mammary tumorigenesis. Gene *172*, 199–205.

Iida-Klein, A., Zhou, H., Lu, S.S., Levine, L.R., Ducayen-Knowles, M., Dempster, D.W., Nieves, J., and Lindsay, R. (2002). Anabolic action of parathyroid hormone is skeletal site specific at the tissue and cellular levels in mice. J. Bone Miner. Res. *17*, 808–816.

Iwaniec, U.T., Wronski, T.J., Liu, J., Rivera, M.F., Arzaga, R.R., Hansen, G., and Brommage, R. (2007). PTH stimulates bone formation in mice deficient in Lrp5. J. Bone Miner. Res. *22*, 394–402.

Jackson, A., Vayssiere, B., Garcia, T., Newell, W., Baron, R., Roman-Roman, S., and Rawadi, G. (2005). Gene array analysis of Wnt-regulated genes in C3H10T1/2 cells. Bone *36*, 585–598.

Jilka, R.L. (2007). Molecular and cellular mechanisms of the anabolic effect of intermittent PTH. Bone *40*, 1434–1446.

Jilka, R.L., Weinstein, R.S., Bellido, T., Roberson, P., Parfitt, A.M., and Manolagas, S.C. (1999). Increased bone formation by prevention of osteoblast apoptosis with parathyroid hormone. J. Clin. Invest. *104*, 439–446.

Kato, M., Patel, M.S., Levasseur, R., Lobov, I., Chang, B.H., Glass, D.A., II, Hartmann, C., Li, L., Hwang, T.H., Brayton, C.F., et al. (2002). Cbfa1-independent decrease in osteoblast proliferation, osteopenia, and persistent embryonic eye vascularization in mice deficient in Lrp5, a Wnt coreceptor. J. Cell Biol. *157*, 303–314.

Keller, H., and Kneissel, M. (2005). SOST is a target gene for PTH in bone. Bone *37*, 148–158.

Kimble, R.B., Srivastava, S., Ross, F.P., Matayoshi, A., and Pacifici, R. (1996). Estrogen deficiency increases the ability of stromal cells to support murine osteoclastogenesis via an interleukin-1and tumor necrosis factor- mediated stimulation of macrophage colony-stimulating factor production. J. Biol. Chem. *271*, 28890–28897.

Kong, Y.Y., Feige, U., Sarosi, I., Bolon, B., Tafuri, A., Morony, S., Capparelli, C., Li, J., Elliott, R., McCabe, S., et al. (1999). Activated T cells regulate bone loss and joint destruction in adjuvant arthritis through osteoprotegerin ligand. Nature *402*, 304–309.

Kulkarni, N.H., Halladay, D.L., Miles, R.R., Gilbert, L.M., Frolik, C.A., Galvin, R.J., Martin, T.J., Gillespie, M.T., and Onyia, J.E. (2005). Effects of parathyroid hormone on Wnt signaling pathway in bone. J. Cell. Biochem. *95*, 1178–1190.

Luo, Q., Kang, Q., Si, W., Jiang, W., Park, J.K., Peng, Y., Li, X., Luu, H.H., Luo, J., Montag, A.G., et al. (2004). Connective tissue growth factor (CTGF) is regulated by Wnt and bone morphogenetic proteins signaling in osteoblast differentiation of mesenchymal stem cells. J. Biol. Chem. *279*, 55958–55968.

Ma, Y.L., Cain, R.L., Halladay, D.L., Yang, X., Zeng, Q., Miles, R.R., Chandrasekhar, S., Martin, T.J., and Onyia, J.E. (2001). Catabolic effects of continuous human PTH (1–38) in vivo is associated with sustained stimulation of RANKL and inhibition of osteoprotegerin and gene-associated bone formation. Endocrinology *142*, 4047–4054.

Moon, R.T., Bowerman, B., Boutros, M., and Perrimon, N. (2002). The promise and perils of Wnt signaling through beta-catenin. Science *296*, 1644–1646.

Neer, R.M., Arnaud, C.D., Zanchetta, J.R., Prince, R., Gaich, G.A., Reginster, J.Y., Hodsman, A.B., Eriksen, E.F., Ish-Shalom, S., Genant, H.K., et al. (2001). Effect of parathyroid hormone (1-34) on fractures and bone mineral density in postmenopausal women with osteoporosis. N. Engl. J. Med. *344*, 1434–1441.

Nishida, S., Yamaguchi, A., Tanizawa, T., Endo, N., Mashiba, T., Uchiyama, Y., Suda, T., Yoshiki, S., and Takahashi, H.E. (1994). Increased bone formation by intermittent parathyroid hormone administration is due to the stimulation of proliferation and differentiation of osteoprogenitor cells in bone marrow. Bone *15*, 717–723.

Ouji, Y., Yoshikawa, M., Shiroi, A., and Ishizaka, S. (2006). Wnt-10b secreted from lymphocytes promotes differentiation of skin epithelial cells. Biochem. Biophys. Res. Commun. *342*, 1063–1069.

Pettway, G.J., Schneider, A., Koh, A.J., Widjaja, E., Morris, M.D., Meganck, J.A., Goldstein, S.A., and McCauley, L.K. (2005). Anabolic actions of PTH (1-34): use of a novel tissue engineering model to investigate temporal effects on bone. Bone *36*, 959–970.

Pettway, G.J., Meganck, J.A., Koh, A.J., Keller, E.T., Goldstein, S.A., and McCauley, L.K. (2007). Parathyroid hormone mediates bone growth through the regulation of osteoblast proliferation and differentiation. Bone *42*, 806–818.

Potts, J. (1998). Primary hyperparathyroidism. In Metabolic Bone Diseases. L.V.A.a, S. Krane, ed. (San Diego: Academic Press), pp. 411–442.

Qin, L., Qiu, P., Wang, L., Li, X., Swarthout, J.T., Soteropoulos, P., Tolias, P., and Partridge, N.C. (2003). Gene expression profiles and transcription factors involved in parathyroid hormone signaling in osteoblasts revealed by microarray and bioinformatics. J. Biol. Chem. *278*, 19723–19731.

Qin, L., Raggatt, L.J., and Partridge, N.C. (2004). Parathyroid hormone: a double-edged sword for bone metabolism. Trends Endocrinol. Metab. *15*, 60–65.

Rawadi, G., Vayssiere, B., Dunn, F., Baron, R., and Roman-Roman, S. (2003). BMP-2 controls alkaline phosphatase expression and osteoblast mineralization by a Wnt autocrine loop. J. Bone Miner. Res. *18*, 1842–1853.

Rifas, L., Arackal, S., and Weitzmann, M.N. (2003). Inflammatory T cells rapidly induce differentiation of human bone marrow stromal cells into mature osteoblasts. J. Cell. Biochem. *88*, 650–659.

Robertson, G., Xie, C., Chen, D., Awad, H., Schwarz, E.M., O'Keefe, R.J., Guldberg, R.E., and Zhang, X. (2006). Alteration of femoral bone morphology and density in COX-2−/− mice. Bone *39*, 767–772.

Roggia, C., Gao, Y., Cenci, S., Weitzmann, M.N., Toraldo, G., Isaia, G., and Pacifici, R. (2001). Up-regulation of TNF-producing T cells in the bone marrow: A key mechanism by which estrogen deficiency induces bone loss in vivo. Proc. Natl. Acad. Sci. USA *98*, 13960–13965.

Sawakami, K., Robling, A.G., Ai, M., Pitner, N.D., Liu, D., Warden, S.J., Li, J., Maye, P., Rowe, D.W., Duncan, R.L., et al. (2006). The Wnt co-receptor LRP5 is essential for skeletal mechanotransduction but not for the anabolic bone response to parathyroid hormone treatment. J. Biol. Chem. *281*, 23698–23711.

Schmidt, I.U., Dobnig, H., and Turner, R.T. (1995). Intermittent parathyroid hormone treatment increases osteoblast number, steady state messenger ribonucleic acid levels for osteocalcin, and bone formation in tibial metaphysis of hypophysectomized female rats. Endocrinology *136*, 5127–5134.

Spencer, G.J., Utting, J.C., Etheridge, S.L., Arnett, T.R., and Genever, P.G. (2006). Wnt signalling in osteoblasts regulates expression of the receptor activator of NFkappaB ligand and inhibits osteoclastogenesis in vitro. J. Cell Sci. *119*, 1283–1296.

Stojceva-Taneva, O., Fadda, G.Z., Smogorzewski, M., and Massry, S.G. (1993). Parathyroid hormone increases cytosolic calcium of thymocytes. Nephron *64*, 592–599.

Tobimatsu, T., Kaji, H., Sowa, H., Naito, J., Canaff, L., Hendy, G.N., Sugimoto, T., and Chihara, K. (2006). Parathyroid hormone increases beta-catenin levels through Smad3 in mouse osteoblastic cells. Endocrinology *147*, 2583–2590.

Vaes, B.L., Dechering, K.J., van Someren, E.P., Hendriks, J.M., van de Ven, C.J., Feijen, A., Mummery, C.L., Reinders, M.J., Olijve, W., van Zoelen, E.J., and Steegenga, W.T. (2005). Microarray analysis reveals expression regulation of Wnt antagonists in differentiating osteoblasts. Bone *36*, 803–811.

Wan, M., Yang, C., Li, J., Wu, X., Yuan, H., Ma, H., He, X., Nie, S., Chang, C., and Cao, X. (2008). Parathyroid hormone signaling through low-density lipoprotein-related protein 6. Genes Dev. *22*, 2968–2979.

Yadav, V.K., Ryu, J.H., Suda, N., Tanaka, K.F., Gingrich, J.A., Schutz, G., Glorieux, F.H., Chiang, C.Y., Zajac, J.D., Insogna, K.L., et al. (2008). Lrp5 controls bone formation by inhibiting serotonin synthesis in the duodenum. Cell *135*, 825–837.

Zaidi, M. (2007). Skeletal remodeling in health and disease. Nat. Med. *13*, 791–801.